Alternative 4D Trajectories for the avoidance of weather- and contrail-sensitive volumes

Raúl Sáez
Department of Physics - Aerospace division
Technical University of Catalonia (UPC)
Castelldefels, Spain
International Centre for Numerical Methods in Engineering (CIMNE)
Barcelona, Spain
raul.saez.garcia@upc.edu

Bryan G. Cabrera, Marc Melgosa and Xavier Prats
Department of Physics - Aerospace division
Technical University of Catalonia (UPC)
Castelldefels, Spain

Angelo Riccio
Science & Technology Department
Università degli Studi di Napoli Parthenope (UNIPARTH)
Naples, Italy

René Verbeek and Nick van den Dungen
Air Traffic Management & Airport Operations
Royal Netherlands Aerospace Centre (NLR)
Amsterdam, Netherlands

Abstract*—We present a framework to generate, in a multi-aircraft environment, 4D optimized trajectories in a scenario with several weather constraints obtained with advanced weather prediction models. We focus on the trajectory optimization module of this framework, which is based on a point-mass representation of the aircraft. By tuning some of the parameters of this module, we compute several alternative trajectories avoiding these constraints both laterally and vertically. The experiment conducted involves flights crossing the North Atlantic region, while in the en-route phase. This preliminary framework is also used to run the experiments in multiple cycles or consecutive time periods, assuming different update times for the weather constraints, and choosing the best trajectory per flight and per cycle. The ultimate goal of the framework is to develop innovative procedures in the air traffic management system to reduce the climate and environmental impact of aviation, while increasing the resilience of air operations to weather phenomena.*

***Keywords*—Trajectory Optimization, Environment, Weather Avoidance**

I. Introduction

Weather phenomena are one of the biggest causes for significant delays and unpredictable disruptions in air traffic management (ATM) network operations. Weather is also one of the main causes of aviation accidents. In addition, the changing global climate will probably increase the future severity and frequency of these air-traffic-disturbing weather phenomena. Besides airspace or airport capacity, these situations deteriorate the predictability of 4-dimensional (4D) trajectories within the ATM network and increase the delays of the operations. Furthermore, aviation itself has a responsibility to mitigate its climate impact and; to improve the long-term sustainability of the ATM operations; and to contribute to the global effort towards the reduction of climate change.

In this context, in a previous work [1], the authors presented an integrated trajectory optimization framework (depicted in Figure 1) to tactically define environmentally-scored optimal 4D trajectories, for a multi-aircraft airspace configuration, using advanced numerical weather prediction models, and combined with air traffic control (ATC) driven demand-capacity balancing methods. In the setup proposed in [1], a set of alternative trajectories avoiding weather- and contrail-sensitive areas are computed by each aircraft onboard and downlinked to the ATC. Then, a ground-support tool (the trajectory selector module in Figure 1) is used to select the best trajectory per aircraft. In the current paper, we present a proof of concept of some of the elements previously described in [1], mainly focusing on the optimisation of aircraft trajectories. We give further details of some of the modules of our framework, in charge of computing, by solving an optimal control problem for consecutive time periods, a series of alternative trajectories avoiding several weather constraints.

Differently from (on-going) related research—which mainly focuses on the dispatch of individual trajectories and/or on air traffic flow management enhancements—the main contribution of our solution is the consideration of the following aspects into a unique problem: i) weather-resilient 4D trajectory (re)planning for the flight execution phase, tackling (near) real-time aspects; ii) consideration of network and safety constraints by optimizing the overall set of concerned trajectories in the area of interest; and iii) an environmentally-scored decision making algorithm intended to work in a hypothetical

*The work presented in this paper has received funding from the SESAR Joint Undertaking (JU) under grant agreement No 890898, corresponding to the project "Innovative Operations and Climate and Weather Models to Improve ATM Resilience and Reduce Impacts" (SESAR-H2020-ER4 CREATE) within the European Union's Horizon 2020 research and innovation program. The opinions expressed herein reflect the authors view only. Under no circumstances shall the SESAR JU be responsible for any use that may be made of the information contained herein.

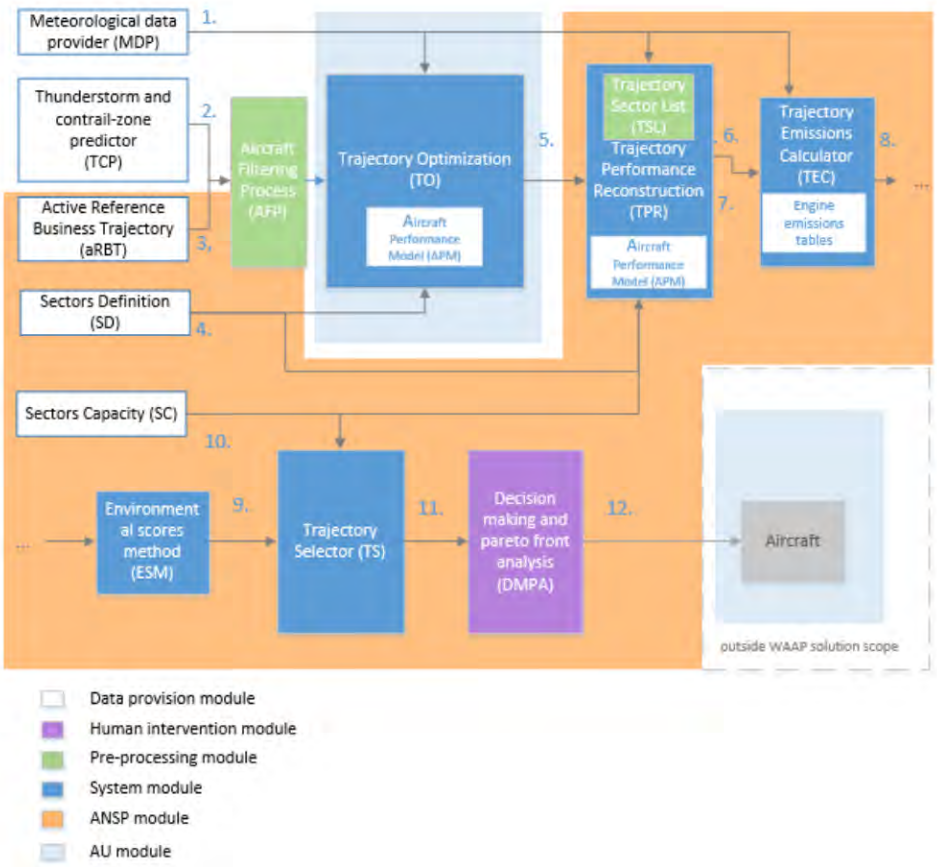

Fig. 1. Framework modules diagram

ATC decision support tool (DST). The ultimate goal of the proposed framework is to develop innovative procedures in the ATM system to reduce the climate and environmental impact of aviation, while increasing the resilience of air operations to weather phenomena.

Similar works have dealt with the optimization of trajectories to avoid weather constraints while considering several environmental parameters in the objective function, like [2]. More recently, other works have focused on more sophisticated thunderstorm models to set up an optimal control problem used to generate trajectories avoiding unpredictable convective weather [3]. However, as aforementioned, in these works only one trajectory was considered at a time and at the planning stage of the flight, thus, disregarding multi-aircraft scenarios in the execution phase of the flight.

Other tools like the Traffic Aware Strategic Aircrew Requests (TASAR) [4] system proposed by NASA, rely on a similar concept of operations as the one proposed in this paper. However, the potential updates in the planned trajectories focus only on efficiency gains from the point of view of individual trajectories, and without necessarily considering the environmental effects in the different airspace volumes.

II. Background

One of the requirements for our framework to work as intended is having good-quality weather data. Indeed, one of the crucial factors that significantly affects airline operations is weather, so it is important to have the most accurate data available. Weather conditions are one of the main causes of flight delays, cancelled flights and, in the worst case scenario, accidents. Among the weather phenomena causing disruptions in airline transportation, one can list: limited visibility, thunderstorms (with associated severe turbulence, lightning, heavy precipitation, hail), strong wind (with associated wind shear), icing and snowfall [5]. According to the European Organisation for the Safety of Air Navigation [6], the average delay in 2019 caused by adverse weather conditions in Europe was 0.5 min per flight.

Numerical Weather Prediction (NWP) models and numerous post-processing tools have been developed to diagnose severe weather conditions, potentially disruptive for aviation operations, on both nowcast (lead times < 3 h) and forecast (> 3 h) times. In this work, we used the WRF (Weather and Research Forecast) model [7], augmented with the Air Force Weather Agency (AFWA) diagnostic module [8], from which we estimated CAPE (Convective Available Potential Energy) and precipitation as a proxy for thunderstorm detection [9],

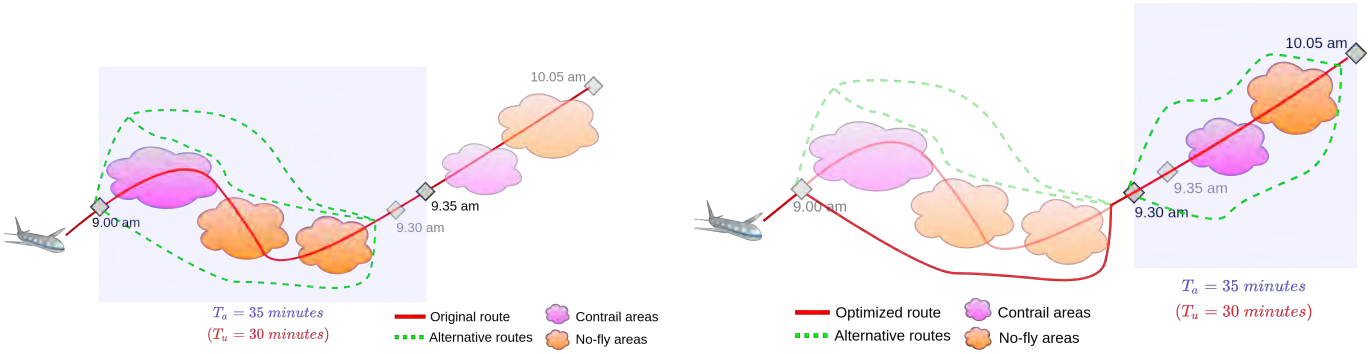

(a) 1st time period

(b) 2nd time period

Fig. 2. Alternative trajectories computation for 2 consecutive time periods

temperature and relative humidity values for the contrail-sensitive areas, according to the so-called SAC (Schmidt-Appleman criterion) [10]. v

III. Methodology

In this section, we describe some of the main parts of our framework (part of CREATE, a SESAR Exploratory Research project), mainly focusing on the Trajectory Optimization (TO) module. As a reminder, as explained in [1], this module is just one of the multiple modules that compose our framework (Figure 1).

In this paper, as it will be thoroughly described in Section IV, we present a scenario in which aircraft avoid several weather constraints by flying alternative trajectories. The generation process of these trajectories is described in Section III-A, while in Section III-B we mainly describe the trajectory optimization algorithm used to generate those trajectories.

A. Alternative Trajectories Generation Process

The CREATE framework is based on the repetition of several cycles or iterations for different consecutive time periods, in which one trajectory (among a set of alternative trajectories) is chosen per aircraft depending on the environmental score assigned by the ESM module (Figure 1). Furthermore, sector capacities will be also taken into account when selecting the best trajectory per aircraft.

The aim of the TO module is to generate a set of alternative trajectories avoiding a set of weather constraints, which correspond to contrail-sensitive areas and weather related no-fly areas (e.g., thunderstorms). The general process followed by this module is depicted in Figure 2 and the main steps followed are detailed below:

1) **Original flight plans**: the original flight plans are used to determine the original route (i.e., lateral path, the red path in Figure 2) followed by the aircraft, as well as the departure time. The trajectory optimizer (described in Section III-B) uses this time, the aircraft model and the set of waypoints to generate an optimal trajectory from origin to destination per aircraft.
2) **Time filter and triggering point conditions**: updates on the weather, contrail-sensitive areas and weather related no-fly areas are given with a certain periodicity, corresponding to the update time, T_u. The "active" flights (i.e., flights already flying or departing) are filtered for a given period equal to that update time. For instance, assuming $T_u = 30\ minutes$, we could filter the flights which are active from 9am to 9.30am. Then, the flight conditions (i.e., position, altitude, mass and speed) at the specific time at which the flights are active (i.e., at the triggering point) are obtained. These conditions are obtained from the trajectories generated in the previous step, and they will be the initial conditions required by the trajectory optimizer.
3) **Look-ahead time and active areas**: a certain look-ahead time, T_a, is considered for both the contrail-sensitive areas and weather related no-fly areas, as these areas can change with time (e.g. different sizes or positions). This time is used to obtain those areas that will be considered when optimizing the trajectory at each cycle. This time is equal to $T_u + \Delta t$, where Δt corresponds to a given buffer time to facilitate the optimization of the trajectory (i.e., to facilitate avoiding the several areas). For instance, if $\Delta t = 5\ minutes$ and $T_u = 30\ minutes$, only contrail-sensitive areas and weather related no-fly areas in the next 35 minutes would be considered when optimizing the trajectory. Focusing on Figure 2(a), only areas that are crossed by the original route (i.e., red path) until 9.35 am are considered by the trajectory optimizer.
4) **Generation of alternative trajectories**: for each flight, several trajectories are generated. In the case of weather related no-fly areas, only trajectories avoiding these areas are considered, while in the case of contrail-sensitive areas, the original flight crossing the area is also considered. Furthermore, both weather related no-fly areas and contrail-sensitive areas can be avoided both laterally and vertically.
The trajectory optimization algorithm decouples the computation of the lateral path (i.e., route), which is done in a first stage with a guess altitude and speed; and the vertical profile (i.e., speed and altitude profiles).

For the route optimization, a classical A* algorithm is implemented based on a graph that is automatically generated by the trajectory optimizer module. Once a route is found, the vertical profile is optimized with optimal control techniques. See [11] for more details on the trajectory optimization engine.

When optimizing the lateral path, the alternative routes are obtained by considering different possible graphs (see Figure 3). The nodes of these graphs are waypoints that could potentially be part of the optimized route and in case an area has to be avoided, only the points outside this area will be active.

In fact, the different avoidance areas are convexified, as shown in Figure 4. This modification of the original avoidance area ensures that no excessive turns are performed when avoiding these areas. Aircraft will fly more operationally sound trajectories that will not approach them unnecessarily to the areas boundaries.

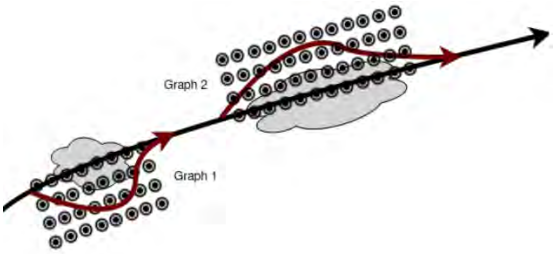

Fig. 3. Dynamic graph generation

The graphs used to optimise the route can be generated in such a way that the trajectory can be forced to divert to the right or to the left of the nominal track, leading to two different families of avoidance trajectories. Then, several buffer values are also used in order to enlarge the avoidance areas (Figure 5), consequently modifying the active points of the aforementioned graphs and thus, obtaining additional alternative trajectories avoiding these areas. In case a trajectory too close to the area is chosen, solutions with a buffered area will be safer.

More details regarding the specific parameters used to determine the alternative trajectories are given in Section IV-A.

5) **Best alternative trajectory and cycle repetition**: once the alternative trajectories are generated, the best alternative trajectory per aircraft has to be chosen. The ESM module (Figure 1) will be responsible for assigning an environmental score to each trajectory. A mixed-integer-linear-programming (MILP) model uses this score to determine the best combination of trajectories from an environmental point of view (and considering also the sectors capacities). As a result of this optimization, one trajectory will be assigned per aircraft. Then, this trajectory will be the one considered by the trajectory optimization module for the next cycle, repeating the process described in steps 1 to 4.

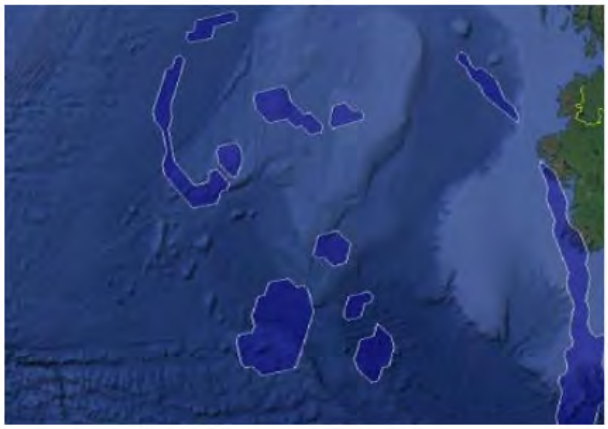

(a) Original areas

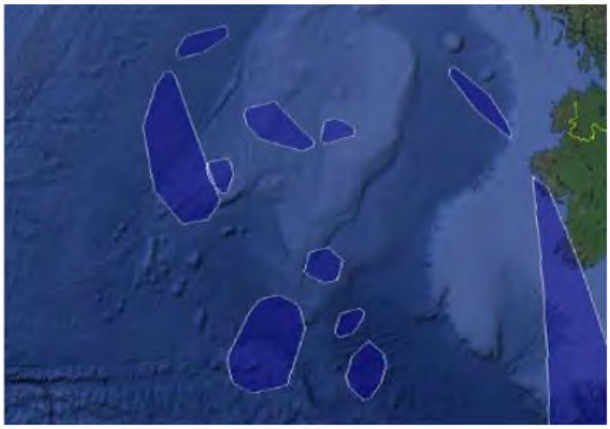

(b) Convexified areas

Fig. 4. Convex areas

Fig. 5. Buffer areas

This paper focuses on the generation of alternative trajectories and is therefore out of the scope to present or discuss the trajectory selection mechanism. Hence, in the results presented in this paper, a random trajectory is chosen among all potential alternatives. In Figure 2(a), the trajectory diverting to the right of the nominal track

is chosen. In this case, this trajectory rejoins the original route before the next cycle (Figure 2(b)).

B. The Aircraft Trajectory Optimization Problem

In the vertical domain, trajectories are generated by solving an optimal control problem, as described in [11]. The aircraft trajectory is divided into N flight phases. Then, for each phase i, defined over the time period $[t_0^{(i)}, t_f^{(i)}]$, a state vector $\boldsymbol{x}^{(i)}(t)$, a control vector $\boldsymbol{u}^{(i)}(t)$ and a parameter vector[1] $\boldsymbol{p}^{(i)}$ are defined. In this paper, the state vector $\boldsymbol{x} = [v, h, s, m]$ is composed by the True Airspeed (TAS), the geometric altitude, the distance to go and the mass of the aircraft; the control vector $\boldsymbol{u} = [T, \gamma, \beta]$ is composed, respectively, by the thrust, the aerodynamic flight path angle and the speed-brakes.

The dynamics of $\boldsymbol{x}$ are expressed by the following set of Ordinary Differential Equations (ODE), considering a point-mass representation of the aircraft reduced to a "gamma-command" model, where vertical equilibrium is assumed:

$$\frac{\mathrm{d}v}{\mathrm{d}t} = \dot{v} = \frac{T(v,h,\pi) - D(v,h,m,\beta)}{m} - g\sin\gamma \tag{1a}$$

$$\frac{\mathrm{d}h}{\mathrm{d}t} = \dot{h} = v\sin\gamma \tag{1b}$$

$$\frac{\mathrm{d}s}{\mathrm{d}t} = \dot{s} = \sqrt{v^2\cos^2\gamma - W_x(s,h)^2} + W_s(s,h) \tag{1c}$$

$$\frac{\mathrm{d}m}{\mathrm{d}t} = \dot{m} = -q(v,h,\pi) \tag{1d}$$

where D is the aerodynamic drag; W_x and W_s are, respectively, the cross and along path wind components; g is the local gravity acceleration; and q is the total fuel flow.

The optimization aims at finding the best control and parameter vectors that minimize the following cost function J, defined over the whole time period $[t_0^{(1)}, t_f^{(N)}]$:

$$J = \int_{t_0^{(1)}}^{t_f^{(N)}} (q(t) + \mathrm{CI})\,\mathrm{d}t \tag{2}$$

where the Cost Index (CI) is a parameter chosen by the operator that reflects the relative importance of the time and fuel costs.

In order to guarantee a feasible and operationally acceptable trajectory, as a result of the optimization, several constraints must be considered. More specifically, the dynamics constraints detailed in Equation (1) have to be met.

In addition, the solution might satisfy some algebraic event constraints setting initial and final conditions at the different phases. These constraints are expressed by non-linear vector functions, and could be used to model restrictions on the initial and/or final CAS, Mach, geometric altitude, pressure altitude, etc. Note that the final event constraints of a certain phase correspond to the initial event constraints of the following one.

Different from the event constraints, which are enforced only at the beginning and/or end of certain phases, algebraic path constraints apply all along the corresponding phase and are expressed by non-linear vector functions of the state, control and parameter variables. Path constraints could be used, for instance, to bound the feasible ground flight path angle (γ_g); or to force it to be constant all along the phase.

In addition, the solution might satisfy simple bounds on the state, control and parameter variables (also known as box constraints). These constraints could be used to bound the aerodynamic flight path angle, to enforce the initial mass or to restrict the maximum allowed thrust, for instance.

As commented before, vertical and lateral optimization are decoupled in our trajectory-optimization framework. Regarding the lateral optimization a graph is used, which is composed of the set of waypoints that could potentially be part of the optimized route, and that form the search space of the A* algorithm. In the particular scenario tackled in this paper, some additional points are added to the graph when areas need to be avoided, as previously explained in Section III-A. Therefore, the aircraft moves from a structured route (i.e., when flying the original route provided in the flight plans) to a free route when avoiding weather related no-fly areas and contrail-sensitive areas.

Finally, it is important to remark the fact that when an area is avoided, the diverting trajectory is designed so as to rejoin the original route. Furthermore, if the triggering point (i.e., the point at which the trajectory is computed, step 2 in Section III-A) of one time period is located in a diverting route computed in a previous time period, the new trajectory will follow the previous diverting route to rejoin the original route.

IV. Results

In this section, we present the results obtained with the CREATE framework presented before, and focusing on the generation of alternative trajectories. In Section IV-A, we present the scenario and case studies tackled in this paper. In Section IV-B, we present the results for all the traffic during one time period, while in Section IV-C and IV-D, we focus on two specific flights to illustrate better the capabilities of our framework.

A. Experimental Setup

In this work, we used flight plans obtained from Eurocontrol's data demand repository (DDR2) [12], which contains information about the trajectories flown in Europe every day. The scenario tackled considers 5,000 flights for July 27, 2018. More specifically, we considered the following case studies:

- **Case study 1**: 5 iterations from 9 am to 11 am with $T_u = 30\ minutes$ and $T_a = 35\ minutes$.
- **Case study 2**: 6 iterations from 4 pm to 6.30 pm with $T_u = 30\ minutes$ and $T_a = 35\ minutes$.

In order to optimize the trajectories, we needed an aircraft performance model, which in this work was obtained from Eurocontrol's Base of Aircraft Data (BADA) version 4 [13]. In the case the aircraft model did not correspond to any of the BADA models, we used a comparable aircraft in terms of performance and physical dimensions of the aircraft.

[1]The parameter vector is formally defined as a vector of variables that are not time dependent

As previously described in Section II, weather data was obtained from NWP models and numerous post-processing tools. More specifically, the following data was used by the trajectory-optimization framework:

- **Pressure, temperature and wind** in NetCDF (Network Common Data Form) format every 30 minutes.
- **Weather related no-fly areas and contrail-sensitive areas** every 30 minutes, defined as polygons with altitude information. A CAPE index $>$ 120 J/kg and a precipitation threshold $>$ 0.3 mm/h were used to obtain the weather related no-fly areas. Figure 6 depicts the weather related no-fly areas for case study 1.

(a) 10am

(b) 10.30am

Fig. 6. Weather related no-fly areas by using CAPE $>$ 120 J/kg and precipitations $>$ 0.3 mm/h (July 27, 2018)

The potential number of alternative trajectories per flight used in this work was 14. The graphs (Section III-A) were configured to force diversion to the right, to the left or allowing either side in those cases where multiple areas had to be avoided. In this experiment, weather-related no-fly areas were only avoided laterally as no cloud-top height information was available. On the other hand, contrail-sensitive areas could also be avoided vertically and the original route was also considered as a candidate trajectory.

B. Results for July 27, 2018

The number of flights considered in each iteration (as described in Section IV-A) was the following:

- Case study 1: 1152, 1160, 1173, 1181, 1183 flights for 9 am, 9.30 am, 10 am, 10.30 am and 11 am, respectively.
- Case study 2: 393, 319, 269, 235, 227 and 153 flights for 4 pm, 4.30 pm, 5 pm, 5.30 pm, 6 pm and 6.30 pm, respectively.

Figure 7 depicts, in red colour, the flights considered in case study 1 at 10 am, together with the weather related no-fly areas location (in dark blue) at that time. Notice that only those areas that are crossed by at least one flight are shown. The cyan section of the trajectories corresponds to the flight location during the time period from 10 am to 10.30 am.

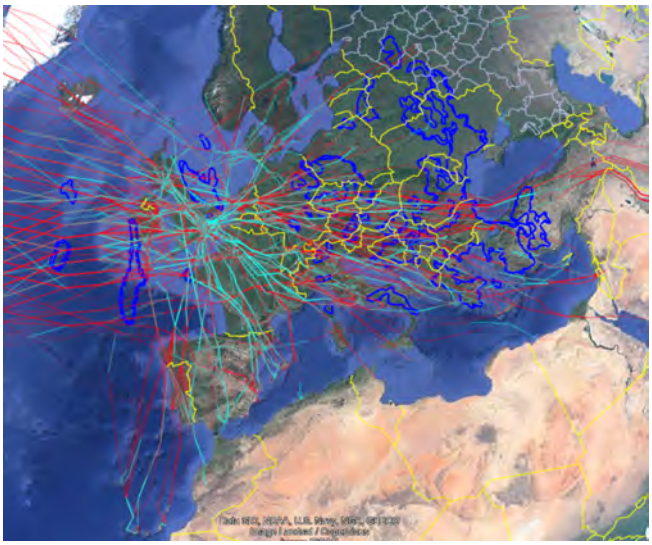

Fig. 7. Trajectories and areas crossed over Europe on July 27, 2018 at 10 am

All computations were made in a laptop computer running Ubuntu 20.04 LTS, with 16GB of RAM memory and an Intel(R) Core(TM) i7-1185G7 @ 3.00GHz processor. It took approximately 2 minutes to generate all the required inputs for the trajectory-optimization framework. The total time to run all the simulations for one time period took a minimum of 3.8 minutes (at 6.30 pm) and a maximum of 54 minutes (at 11 am). It is important to highlight the fact that the current framework is still a prototype, and we intend to improve the computational times in the future. Furthermore, these times are greatly affected by the number of flights and involved areas to be avoided.

Finally, not all the flights could be run successfully. The main reason for this issue is the fact that, for certain time periods, the flights are already located inside a weather related no-fly area. In such a case, it is impossible for the trajectory-optimization framework to compute a trajectory. Additionally, even if the flight is located outside the area but very close to it, the optimizer might not successfully generate a trajectory either. Furthermore, there are areas that are too big for the flight to avoid them properly. Indeed, one of the tasks for future work is to improve the definition of these areas, by tuning some of the parameters used to obtain them, like the CAPE index or the precipitation threshold.

(a) Original route

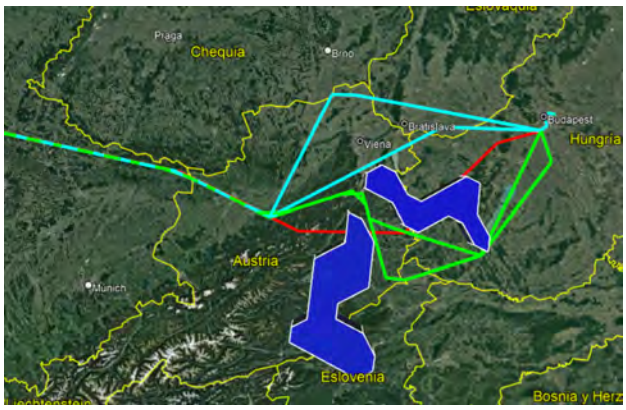

(b) 10am-10.30am

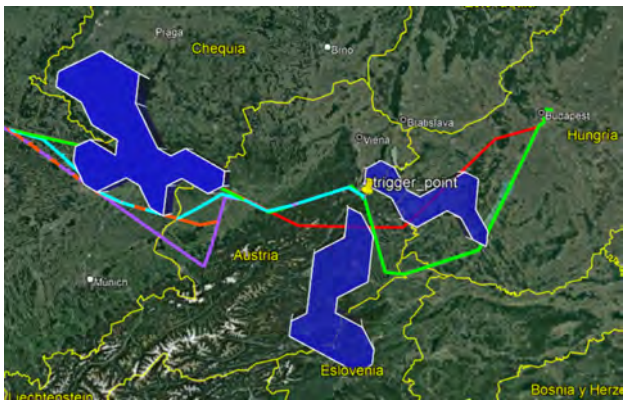

(c) 10.30am-11.00am

Fig. 8. Alternative trajectories for two time periods for flight LOT33 (B787-800) from LHBP to KJFK (July 27, 2018)

C. Alternative Trajectories for Flight LOT33

In order to better observe the output of our framework, in this section we focus on flight LOT33, a Boeing B787-800 flying from Budapest-Ferenc Liszt Airport (LHBP) to John F. Kennedy International Airport (KJFK) on July 27, 2018. We will focus on two iterations of case study 1, from 10 am to 11 am, depicted in Figure 8.

In Figure 8(a), we can see the original route in red. The first iteration, from 10 am to 10.30 am, is depicted in Figure 8(b). As it can be observed, the original route crosses two no-fly areas (in dark blue). In this situation, the trajectory optimizer computes a set of alternative trajectories. 12 alternative trajectories were generated in this case, but only 4 have been depicted in Figure 8(b) to facilitate the visualization of the trajectories. Two diverting to the right (in cyan) and two to the left (in light green). Once the areas are avoided, the trajectories rejoin the original route. The southernmost trajectory is chosen as the best alternative trajectory in this case. In the next iteration, at 10.30 am (Figure 8(c)), the aircraft is still avoiding the areas of the previous iteration. Therefore, the initial flight conditions for the optimizer (at the *trigger_point* in Figure 8(c)) are located at the previously generated trajectory. The aircraft follows that trajectory until the next area to avoid. In this case, it is better to avoid this area diverting to the left. Three trajectories are depicted in this case, coloured in cyan, orange and purple. After avoiding the area, they rejoin, once again, the original route.

D. Alternative Trajectories for Flight UAE161

In this section, we focus on flight UAE161, a Boeing 777-300ER flying from Dubai International Airport (OMDB) to Dublin Airport (EIDW) on July 27, 2018. Figure 9 depicts one of the last sections of this flight, with the triggering point (the cross in Figure 9) located in Germany at 9.00am.

Several areas are depicted in Figure 9: two weather related no-fly areas, T1 and T2, and two contrail-sensitive areas, C1 and C2. Regarding C1, we can observe that it is located very close to the triggering point, which makes it impossible to avoid it either laterally or vertically; the only feasible option is to cross it. On the other hand, C2 can be avoided both vertically by following the blue trajectory and laterally by following the orange trajectory. C2 is only active between FL315 and FL360. When following the blue trajectory, the aircraft climbs to a FL380 in order to avoid the contrail vertically, as shown in the vertical profile in Figure 9.

Regarding T1 and T2, they are both avoided by diverting to the left. Avoiding the thunderstorms to the right would be possible too, but not valid from an operational point of view, as this option would drastically increase the total flight distance.

Another aspect that is worth highlighting is the yellow area surrounding the original flight plan in Figure 9, known as *look-ahead time area*. As explained in Section III, only areas (i.e., no-fly areas and contrail-sensitive areas) intersecting the original flight plan after a given look-ahead time are considered when optimizing the trajectory. The *look-ahead time area* serves the same purpose, but in this case all the areas to be avoided falling within this area will be also considered, not just the ones intersecting the flight plan. This will allow aircraft to avoid in a smarter way the areas, anticipating future diversions and leading to more operational trajectories.

Finally, Figure 10 shows the set of alternative trajectories generated for flight UAE161. We have removed both the weather related no-fly areas and contrail-sensitive areas for a better visibility.

Fig. 9. Alternative trajectories for flight UAE161 (B777-300ER) from OMDB to EIDW (July 27, 2018))

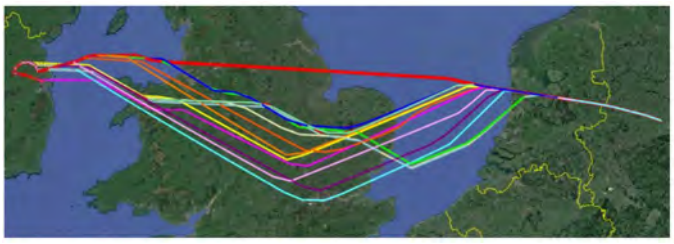

Fig. 10. Alternative trajectories for flight UAE161 (B777-300ER) from OMDB to EIDW (July 27, 2018))

V. Conclusions

In this paper, we have presented some of the functionalities of the CREATE framework, mainly focusing on its trajectory-optimization module. This module is in charge of generating a set of alternative trajectories per flight in a multi-aircraft environment, avoiding weather related no-fly areas and contrail-sensitive areas located in the original flown trajectory. In future publications, we will present the rest of the modules that conform the framework, which focus on the selection of the best alternative trajectory (with a MILP model) depending on an environmental score and by taking into account the capacity of the airspace sectors.

In future work, we are also planning to further investigate the definition of the different no-fly areas, as some of them complicated the trajectory optimizer task of generating potential trajectories. The CAPE index or the precipitation threshold are some of the potential parameters that could be investigated in order to solve these issues. Furthermore, while the computational times are in the order of minutes for thousands of flights, we are also planning to scale our algorithm to further reduce these computational times with the aim of achieving a higher technology readiness level (TRL) solution.

This work is the first step towards the ultimate goal of the CREATE project: to develop innovative procedures in the ATM system to reduce the climate and environmental impact of aviation, while increasing the resilience of air operations to weather phenomena.

References

[1] N. van den Dungen, K. Sutopo, X. Prats, V. di Vito, and A. Riccio, "Multi-aircraft environmentally-scored weather-resilient optimised 4D-trajectories," in *FABEC Research Workshop: Climate change and the role of air traffic control*. Vilnius, Lithuania: FABEC, Sep 2021.

[2] G. Serafino, "Multi-objective aircraft trajectory optimization for weather avoidance and emissions reduction," in *Modelling and Simulation for Autonomous Systems (MESAS)*, 2015.

[3] D. González-Arribas, M. Soler, M. Sanjurjo-Rivo, M. Kamgarpour, and J. Simarro, "Robust aircraft trajectory planning under uncertain convective environments with optimal control and rapidly developing thunderstorms," *Aerospace Science and Technology*, vol. 89, pp. 445–459, 2019.

[4] M. G. Ballin and D. J. Wing, "Traffic Aware Strategic Aircrew Requests (TASAR)," in *12th AIAA Aviation Technology, Integration, and Operations (ATIO) Conference and 14th AIAA/ISSM*. Indianapolis, Indiana, USA: AIAA, Sep 2012.

[5] I. Gultepe, R. Sharman, P. D. Williams, B. Zhou, G. Ellrod, P. Minnis, S. Trier, S. Griffin, S. Yum, B. Gharabaghi *et al.*, "A review of high impact weather for aviation meteorology," *Pure and applied geophysics*, vol. 176, no. 5, pp. 1869–1921, 2019.

[6] C. Walker, "CODA Digest. All-causes delay and cancellations to air transport in Europe. Annual report for 2019," EUROCONTROL, Tech. Rep., 2020.

[7] W. C. Skamarock, J. B. Klemp, J. Dudhia, D. O. Gill, Z. Liu, J. Berner, W. Wang, J. G. Powers, M. G. Duda, D. M. Barker *et al.*, "A description of the advanced research WRF model version 4," National Center for Atmospheric Research: Boulder, CO, USA, Tech. Rep. NCAR/TN-556+STR, 2019.

[8] G. Creighton, E. Kuchera, R. Adams-Selin, J. McCormick, S. Rentschler, and B. Wickard, "AFWA diagnostics in WRF," 2014.

[9] M. Taszarek, S. Kendzierski, and N. Pilguj, "Hazardous weather affecting European airports: Climatological estimates of situations with limited visibility, thunderstorm, low-level wind shear and snowfall from ERA5," *Weather and Climate Extremes*, vol. 28, no. 100243, 2020.

[10] U. Schumann, "On conditions for contrail formation from aircraft exhausts," *Meteorologische Zeitschrift*, vol. 5, pp. 4–23, 1996.

[11] R. Dalmau, M. Melgosa, S. Vilardaga, and X. Prats, "A Fast and Flexible Aircraft Trajectory Predictor and Optimiser for ATM Research Applications," in *8th Proceedings of the International Conference on Research in Air Transportation (ICRAT)*. Castelldefels, Spain: EUROCONTROL and FAA, 2018.

[12] Eurocontrol, *DDR2 Reference Manual for General Users 2.9.4*, 2017.

[13] ——, "User Manual for the Base of Aircraft Data (BADA) Family 4," 2014.